IOP Conf. Series: Materials Science and Engineering **214** (2017) 012007 doi:10.1088/1757-899X/214/1/012007

From Cell to Module: Fabrication and Long-term Stability of Dye-sensitized Solar Cells

N M Nursam[1,]*, J Hidayat[1], L Muliani[1], P N Anggraeni[1], L Retnaningsih[1], and N Idayanti[1]

[1]Research Center for Electronics and Telecommunications, Indonesian Institute of Science, Kompleks LIPI Building 20 Level 4, Cisitu, Bandung – Indonesia 40135

Email: nata002@lipi.go.id

Abstract. Dye-sensitized solar cell (DSSC), which has been firstly developed by Graetzel et al back in 1991, has attracted a considerable interest since its discovery. However, two of the main challenges that the DSSC technology will have to overcome towards commercialization involve device scale-up and long-term stability. In our group, the fabrication technology of DSSC has been developed from laboratory to module scale over the past few years, nevertheless, the long-term stability has still became a major concern. In this contribution, the long-term DSSC performance in relation to their scale-up from cell to module is investigated. The photoelectrode of the DSSCs were fabricated using nanocrystalline titanium dioxide materials that were subsequently sensitized using ruthenium-based dye. Additionally, $TiCl_4$ pre- and post-treatment were carried out to enhance the overall device efficiency. When fabricated as cells, the DSSC prototypes showed relatively stable performance during repeated tests over three months. In order to increase the output power of the solar cells, the DSSCs were then connected in a Z-type series connection to obtain sub-module panels. The DSSC sub-modules exhibit poor stability, particularly as indicated by the significant decrease in the short circuit current (I_{SC}). Herein, the effect of photoelectrode and sealant materials as well as module design are investigated, highlighting their profound influence upon the DSSC efficiency and long-term stability.

1. Introduction

Among various types of solar cells, DSSC combines both the promise of high efficiency and low fabrication cost. Additionally, they can be fabricated over flexible substrate and can offer transparency and workability to be integrated into buildings as smart window, of which those could not be accommodated by the first two generations of photovoltaic technology, that is, the silicon and thin-film based solar cells. Since its breakthrough in 1991 [1], the performance of DSSC has progressed considerably. DSSC with an efficiency of ~13 % has recently been reported by Graetzel and co-workers [2], which constitutes the highest efficiency reported to date. Due to their attractive appearance and affordability reasons, considerable effort has therefore been devoted to enable a commercial upscaling of this type of solar cell.

DSSC panel has been reported to deliver more electricity than the silicon and thin-film solar cells when exposed to low light condition. The upscaling of DSSC therefore holds a promising prospect for commercialization. However, the reports in this area [3-6] have not been as extensive as those reported in the area of cells optimization, with the total number of works almost 100 times lower than the latter [7]. One of the early work on DSSC panel was reported by Kay and Gratzel in 1996 [8], demonstrating the fabrication of six DSSC cells connected to each other on a single FTO substrate with a series connection, showing an overall module efficiency of ~5.3%. Large area DSSC modules or panels often suffer from long-term stability issue and also lack in performance compared to their lab-scale devices. In term of commercial applications, these two major issues are crucial in addition to the power conversion efficiency. As a comparison, most silicon solar cell manufacturers would give a warranty of 80-90% of the initial performance after 20 years of operation. Therefore, as the DSSC technology progress from laboratory bench to practical applications, scalability and durability are the two paramount aspects that need to be tackled.

In this contribution, we present a comparative and stability study of DSSC sub-modules with various sealing materials. To date, little effort has been undertaken to investigate the stability of DSSC modules in relation to the selection of sealant materials. For instance, Sommeling *et al.* [5] and Kato *et al.*[4] reported the effects of electrolyte compositions and types upon the long-term performance of DSSC cells, respectively, whereas Sastrawan and co-workers [9] reported the long-term stability of glass-frit sealed DSSC modules without comparing with other types of sealant. The main functions of the sealing materials in DSSC are to protect the conductor grid (typically, in the form of silver) from the highly reactive electrolyte and to prevent any leaking of electrolytes between the neighboring cells or toward out of the module. Ideally, the sealing material must be chemically inert against the I^-/I_3^- redox couple, while maintain its mechanical and chemical stability under various testing conditions.

2. Experimental Section

2.1. Photoelectrode and Counter-electrode Preparation

The photoelectrode and counter-electrode of the DSSC sub-modules were fabricated on fluorine-doped tin oxide (FTO) coated glass with a conductivity of 15 Ω/sq. First, a diamond cutter was used to remove the FTO layer on the photoelectrode side following the module design as shown in Figure 1. All of the FTO glasses were cleaned by ultrasonicating in soap water, isopropanol and ethanol, consecutively, for 10 min. The TiO_2 paste (Dyesol 18NR-AO) was deposited on the photoelectrode two times using screen printing method (Nylon #325 mesh) to obtain TiO_2 films with a thickness of 8-10 μm. The active area for each sub-module was 2×5 cm^2. Each sub-module consists of two individual cells. All samples were dried in an oven at 100 °C for 10 min between each deposition and then annealed in conveyer belt furnace (Radiant Technology Corporation) at 500 °C for 15 min. All samples then received $TiCl_4$ post-treatment by heating in 40 mM $TiCl_4$ solution at 70 °C for 30 min, followed by another calcination at 500 °C for 15 min. After cooling, the TiO_2 film coated FTO were soaked in Z907 dye solution ($C_{42}H_{52}N_6O_4RuS_2$, Dyesol) in ethanol (20 mg/100 mL) overnight. Before cell construction, the sensitized samples were rinsed thoroughly in ethanol to remove any excess dyes and then dried naturally. All samples turned to maroon color after the immersion.

For the preparation of the counter electrode, the pre-drilled FTO substrates were sputtered with platina target using DC-sputtering process. The coating process was carried out for 20 min with a power of 5 W, initial pressure of 6.6×10^{-3} Pa, argon gas pressure of 5.3×10^{-1} Pa, and rotation speed of 5 rpm.

2.2. Module Assembly

Figure 1 shows the schematic design of the sub-module configuration used in this work. All of the sub-modules were assembled using Z-type series connection, wherein each sub-module comprised of two cells with an active area of 1×5 cm^2. There were three types of module assembled in this work that were categorized according to the type of sealant material. The sealing compounds were printed in both electrodes through a stainless steel screen with #200 mesh. In the first sub-module, namely Module A, the sub-module was sealed using hermetic sealing compound or also known as glass frit (Dyesol), which was made from a mixture of part A and part B with weight compositions of 4:3, 4:2 and 4:1 (see Table 1 for details). These sub-modules were labeled as Module A1, A2 and A3, respectively. Meanwhile, the sealing compound in Module B consisted of Amosil 4R and Amosil 4H

(Solaronix) with weight ratios of 1:1, 4:3 and 4:2 (Table 1). These sub-modules were labeled as Module B1, B2 and B3, respectively. In Module C, a commercial silicone rubber sealant was printed without any additives. Then, silver paste (Hunan LEED Electronics, Inc. Co. Ltd.) was coated into each electrode. Both sealant and silver paste were printed with a line-width of 1 mm, while the gaps between the neighboring lines were maintained at approximately 0.3 mm.

Table 1. Mass compositions used for the sealing materials used for DSSC sub-modules

No.	Glass frit		Amosil		Silicon rubber
	Part A (g)	Part B (gr)	4R (g)	4H (g)	
1.	0.500	0.375	0.500	0.500	
2.	0.500	0.250	0.500	0.375	used as is
3.	0.500	0.125	0.500	0.250	

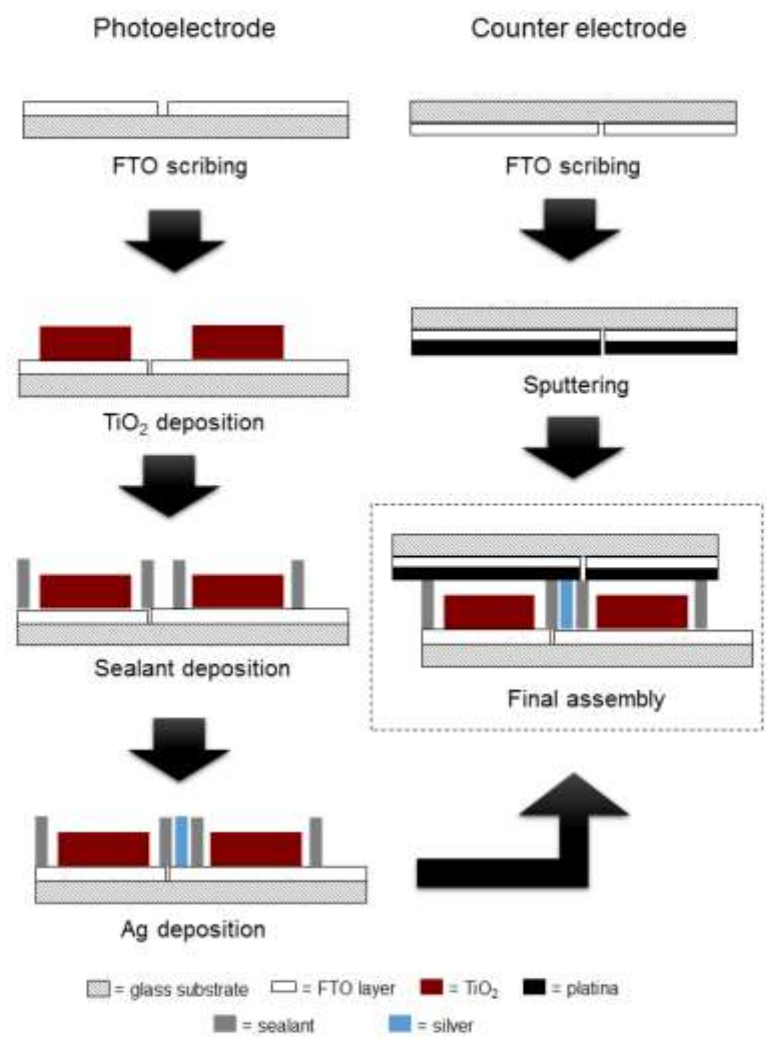

Figure 1. Schematic drawing of the assembly process of DSSC sub-modules.

Both electrodes were subsequently pressed together using paper clip to strengthen the bonding overnight. Once the electrodes have been strongly attached to each other, liquid electrolyte EL-HPE (Dyesol) was injected through the pre-drilled holes. Finally, all of the pre-drilled holes were sealed with glass frit and left to solidify in air. In order to compare the long-term performance of DSSC cell and sub-module, a single cell was prepared following the same procedures as above. The fabrication of this cell can be found elsewhere [10]. This cell was subsequently assembled and sealed using hot melt foil with a thickness of 50 μm (Surlyn, Dyesol). The sealing process was followed by heating the sample at 120 °C for 35 min to melt the foil and to make both electrodes adhered to each other.

2.3. Characterization

The current-voltage (*I-V*) characteristics of sub-modules were measured using a National Instrument source meter under AM1.5G solar simulator (Oriel, Newport USA) and analyzed using Lab-View software. The irradiation intensity was 500 W/m^2 at 25 °C. The efficiency of the cell and sub-modules was determined using the following equation:

$$\eta = \frac{V_{OC} I_{SC} FF}{P_{in}} \times 100\%$$

where V_{OC} and I_{SC} are the open circuit voltage and the short circuit current, respectively, FF is the fill factor, and P_{in} is the power input received during the illumination.

3. Results and Discussion

In this work, hermetic sealing compound (also known as glass frit), Amosil, and silicon rubber was chosen instead of widely used Surlyn hot melt foil due to two reasons. First, the application of glass frit in epoxy form upon large area module is more feasible as it can be deposited using screen printing method. Contrarily, the use of Surlyn would require high precision during the cutting and attachment following the desired pattern. It should be noted, however, that the printing of glass frit needs to be carried out as quickly as possible to avoid fast solidification of the compound. The second reason is related to thermal stability. As Surlyn has low melting point, it will not withstand any high temperature test above 60 °C, thus, glass frit offers better temperature resistibility. Likewise, Amosil and silicone rubber also could stand high temperature (i.e. up to 300 °C), thus rendering them as better sealant than Surlyn. In addition, glass frit, Amosil and silicon rubber can be cured at room temperature, thus avoiding the need for a heating that may degrade the organic components existing in the dye materials. The glass frit and Amosil were opaque-grey in color, while the silicon rubber sealant was transparent.

The photograph of the sub-modules fabricated herein is displayed in Figure 2. All of the sub-modules were opaque and have similar appearance apart from the sealant materials. Figure 3 shows the *I-V* curves of all samples measured on the first day, that is, one day after the assembly has been completed. The corresponding *I-V* parameters are summarized in Table 2. It can be seen that the sub-module fabricated using Amosil demonstrated superior performances compared to the rest of the sub-modules. This was indicated by their average photovoltaic efficiency that was higher than 3 %, regardless of the different element compositions. Overall, the sub-module assembled using silicon rubber and glass frit with 4:1 ratio showed the lowest efficiency. It was suspected that the incomplete curing process was likely to be the reason for such poor performances, which was specifically attributed by the low current generation. The incomplete sealant hardening process may have caused the electrolyte to react with the sealant materials, thus causing insufficient regeneration of the redox components. Moreover, there were higher chance of electrolyte leaking and reacting with silver, thus hampering charge collection and rendering low output current.

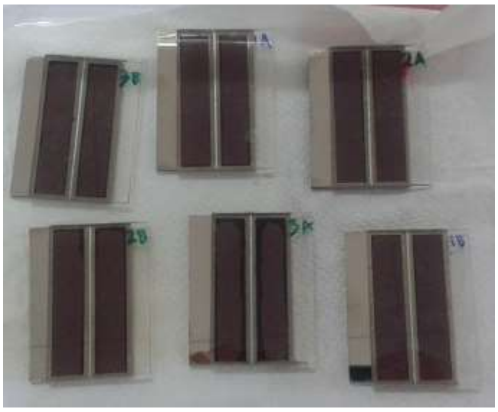

Figure 2. Photograph of the sub-modules sealed with glass frit and Amosil.

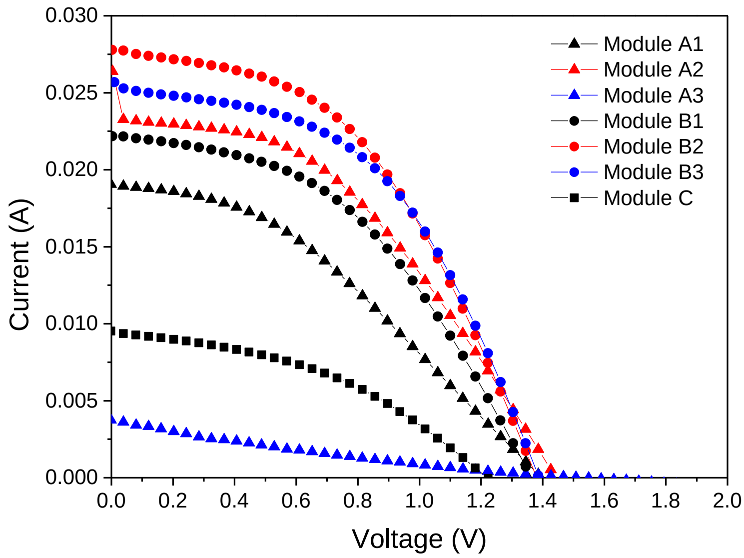

Figure 3. *I-V* curves of the sub-modules assembled using various sealant materials.

Table 2. Electrical characteristics of the sub-modules as measured using *I-V* measurement

Parameter	Glass Frit			Amosil			Silicon rubber
	A1	A2	A3	B1	B2	B3	
P_{max} (watt)	0.009	0.014	0.001	0.014	0.018	0.017	0.005
V_{mp} (volt)	0.733	0.815	0.651	0.815	0.855	0.896	0.733
I_{mp} (ampere)	0.013	0.018	0.002	0.017	0.021	0.019	0.007
FF	0.373	0.384	0.202	0.408	0.379	0.401	0.429
η (%)	1.962	2.918	0.221	2.716	3.579	3.478	0.939

For the long-term stability test, the I-V curves were measured after storing the samples in petri dishes for one week at room temperature without controlling the humidity. It can be seen in Figure 4 that most of the sub-modules were substantially deteriorated, especially when compared to the single cell sample that only suffered from less than 10% reduction in efficiency after one week and was relatively stable after more than 60 days of observation (see inset in Figure 4). Compared to a cell, there are more complicated factors that could attribute to the very low device stability in a module. A single DSC cell does not contain any current collecting component, i.e. silver, that is required to connect the adjacent cells. Thus, there is lower possibility of corrosion. Contrarily, the selection of sealant material in a module is very crucial as the sealant should be able to protect the silver from the electrolyte, in addition to prevent the electrolyte from leaking out. The trend that shows significant decrease in the efficiency (as shown in Figure 4) indicates that both Amosil and silicon rubber could not provide a good sealing ability. The poor stability shown by the sub-modules sealed either with Amosil or silicon rubber was attributed to the electrolyte leaking. This was apparent from the photograph in Figure 5. A visual inspection revealed that there were distinct discolorations around the edges of the sealing, indicating electrolyte depletion in those areas.

From the comparison of the relative η (that is η from day 7 divided by the η_0), the sub-module that was sealed using glass frit with 4:3 ratio demonstrated the best stability out of all samples with an efficiency decrease of approximately 26 % after one week of storage. There is also an indication that the decrease in glass frit part B tends to decrease the long-term stability of the module, and contrarily, the decrease in Amosil 4H tends to increase the long-term stability of the module. However, further tests with more variations in the glass frit and Amosil compositions will be required to confirm these trends. There were also no specific trends showing that the best performing sub-module in the initial measurement consistently showed the best performance after one week. This suggests that the photovoltaic output does not necessarily correlate with the long-term stability. Overall, the sub-modules that were prepared using Amosil have shown the most superior performance, but the best stability was achieved by the sub-modules containing glass frit with 4:3 ratio.

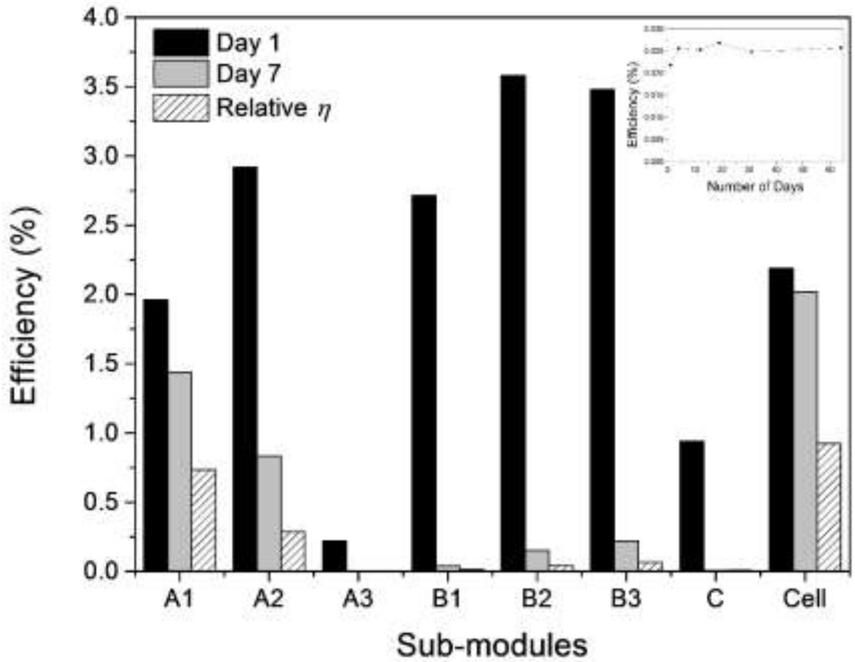

Figure 4. Comparison between the efficiency of sub-modules with various sealant and single cell with Surlyn as the sealant material. The efficiency was also compared on the first day of the assembly (black bars) and after 1 week (patterned bars). The relative η was obtained as a ratio between the efficiency from day 7 and day 1. The time-dependant efficiency of the single cell is shown in the inset.

Figure 5. Photograph showing electrolyte leaking observed in the sub-module sealed with Amosil with 1:1 ratio.

4. Conclusions

Dye-sensitized solar cell (DSSC) sub-modules were fabricated using various sealant materials and tested after one-week storage to monitor their stability. A single cell sealed with hot melt foil was also fabricated as an additional comparison. It was shown that the use of glass frit, Amosil and silicon rubber sealant is applicable for the upscaling of DSSC from cell size to sub-modules with a total active area of 2×5 cm^2. The main technology used for the deposition of the sealant was screen printing, proving that this technology is a low-cost yet facile technique that fully supports the upscaling of DSSC.

During the first *I-V* measurement, the sub-modules sealed with Amosil showed superior performances compared to that of sub-modules sealed with glass frit and silicon rubber. Second measurements carried out after one week of storage, however, revealed that the sub-modules sealed with glass frit demonstrated better stability with the least degradation in the sub-module's efficiency. Electrolyte leaking was suspected as the main culprit for the deterioration. In contrary, the single cell sealed with hot melt foil showed a relatively stable performance. Our study showed that the encapsulation quality of glass frit, Amosil and silicon rubber still are still incomparable with the hot melt foil, although the latter has been proven to be difficult for DSSC upscaling. Thus, further study to optimise the glass frit composition as well as finding the appropriate treatment for glass frit is required to further improve the long-term stability of DSSC modules.

References

[1] O'Regan B and M Graetzel 1991 *Nature* **353** 737
[2] Mathew S, A Yella, P Gao, R Humphrey-Baker, B F E Curchod, and N Ashari-Astani 2014 *Nat. Chem* **6** 242
[3] Hinsch A, J M Kroon, R Kern, I Uhlendorf, J Holzbock, A Meyer*, et al.* 2001 *Prog. Photovoltaics Res. Appl* **9** 425
[4] Kato N, K Higuchi, H Tanaka, J Nakajima, T Sano, and T Toyoda 2011 *Sol. Energy Mater. Sol. Cells* **95** 301
[5] Sommeling P M, M Spath, H J P Smit, N J Bakker, and J M Kroon 2004 *J. Photochem. Photobiol. A* **164** 137
[6] Xue G, Y Guo, T Yu, J Guan, X Yu, J Zhang*, et al.* 2012 *Int. J. Electrochem. Sci* **7** 1496

[7] Fakharuddin A, R Jose, T M Brown, F Fabregat-Santiago, and J Bisquert 2014 *Energy Environ. Sci* **7** 3952
[8] Kay A and M Graetzel 1996 *Sol. Energy Mater. Sol. Cells* **44** 99
[9] Sastrawan R, J Beier, U Belledin, S Hemming, A Hinsch, R Kern, *et al.* 2006 *Sol. Energy Mater. Sol. Cells* **90** 1680
[10] Nursam N M, L Muliani, and J Hidayat 2011 *Jurnal Teknologi Indonesia* **34** 85